Hindawi
International Journal of Optics
Volume 2023, Article ID 8685686, 9 pages
https://doi.org/10.1155/2023/8685686

Research Article

Integrated Free-Space Optics and Fiber Optic Network Performance Enhancement for Sustaining 5G High Capacity Communications

Meshari Alsharari,[1] Khaled Aliqab,[1] Farman Ali,[2] and Ammar Armghan[1]

[1]*Department of Electrical Engineering, College of Engineering, Jouf University, Sakaka 72388, Saudi Arabia*
[2]*Department of Electrical Engineering, Qurtuba University of Science and IT, Dera Ismail Khan 29050, Pakistan*

Correspondence should be addressed to Meshari Alsharari; mmaalsharari@ju.edu.sa and Farman Ali; drfarmanali.optics@qurtuba.edu.pk

Received 4 July 2022; Revised 23 November 2022; Accepted 9 December 2022; Published 13 January 2023

Academic Editor: Rujiang Li

In this paper, the integrated free-space optics (FSO) and fiber optic model is evaluated using new radio (NR) sub-THz link to sustain next generation 5G capacity. The proposed integrated model effectively applies over 25 km single mode fiber, 0.5 m RF wireless, and 500 m optical wireless. In addition, four different sub-THz frequencies (125, 150, 175, and 200 GHz) are estimated on NR-based 5G FSO network, including 22 Gbps 64quadrature amplitude modulation-orthogonal frequency division multiplexing (64QAM-OFDM) signal speed. The proposed FSO enabled fiber optic system is also measured mathematically to satisfy the data transmission accuracy. For confirmation, the theoretical approach of the presented FSO and fiber optic network is realized with an aggregate 342 Gbps speed (16×22). The performance metrics comprising forward error limit (FEL), bit error rate (BER), and error vector magnitude (EVM) are used for weighing simulation results. The outlets of an integrated fiber-FSO network show that by applying NR 5G sub-THz, a high data rate with multiple inputs and multiple outputs (MIMO) transmission capacity can be adjusted victoriously.

1. Introduction

Looking ahead, it is evident that we are steadily going towards new technologies like the Internet of Everything, driverless vehicles, mixed reality, and ultra-high resolution video conferencing. However, the throughput, reliability, and latency requirements will have to meet increasingly demanding criteria due to these new uses. Due to recent advancements in sub-terahertz (sub-THz) technology, researchers are pushing the 5G new radio (NR) to a higher band, particularly the sub-THz spectrum stretching between 100 to 300 GHz, as mentioned in Figure 1 [1–3]. 5G NR connection in the sub-THz band is gaining popularity due to its high data rates. The sub-THz range has the high frequencies required to greatly boost data speeds. Due to its high-frequency properties, the sub-THz band is well suited for many new 5G applications that require huge data speeds. The 5G NR sub-THz communication's high-frequency characteristic allows for the delivery of large amounts of data over short distances [4, 5, 6]. The wireless transmission range is however constrained by the substantial air loss transmission window of 5G NR sub-THz communication. 5G is suitable for densely populated areas because of its sub-THz communication constraints. Since 5G sub-THz connectivity cannot transmit a signal through long-range wireless transmission, it is not the best solution in sparsely populated areas. Given the growing growth of MMW communications, researchers have naturally explored for additional high-frequency bands, particularly the sub-terahertz (sub-THz) band, which is located above the millimeter-wave (MMW) band. Due to their vast bandwidth, the sub-THz spectrum can be utilised in a variety of

Figure 1: Mixed FSO and optical network based framework for addressing the FSO pointing and cochannel interference.

developing applications that require high access data rates [7, 8]. Due to its characteristics, MMW and sub-THz communications can provide high data speeds across short distances. The limitations of 5G NR communications in the MMW and sub-THz bands make them better suited for short-range wireless transmission than long-range wireless transmission. A different kind of wireless transmission technique is called free-space optical (FSO) communication. FSO communication has drawn a lot of interest as a potential solution to the problem of short-range 5G wireless communications [8–10]. A promising approach to achieving the goals of high transmission capacity and long-haul transmission is to aim the transmission rates at many tens of Gb/s using an integrated fiber optics and FSO-based 5G NR system for the simultaneous transmission of 5G MMW and sub-THz signals. The integrated fiber optic and FSO-enabled 5G NR system has the capabilities of high transmission capacity, high access data rates, long-haul transmissions, and vast service regions by combining long-reachfiber-FSO convergence with short-range 5G wireless extension. This paper proposes and experimentally validates the integrated fiber optics and FSO-based 5G NR model for the simultaneous transmission of 5G MMW and sub-THz signals. We simultaneously broadcast signals in the 125, 150, 175, and 200 GHz sub-THz bands using 64-quadrature amplitude modulation (QAM) and orthogonal frequency-division multiplexing (OFDM).

1.1. Previous Work and Background. Different algorithms and strategies to enhance FSO performance have been presented by numerous research organisations from all over the world. The authors demonstrate recent advancements in FSO technology and the variables that affect the interpretation of the results in [11]. The study in [12] assesses the effectiveness of the FSO system across a range of geographic regions. Digital signal processing (DSP) and orthogonal frequency division multiplexing (OFDM) techniques are used to reduce the channel-induced restrictions. Full duplex and all FSO transceivers were recommended by Li et al. [13], who also assessed the performance of the system. In [14], the quality factor and electrical power for FSO lines were explored, and simulation assessments were carried out using OptiSystem. In [15], the bit error rate (BER) of an intensity modulation and direct modulation (IM/DD) FSO link was examined. The OFDM mode division multiplexing (OFDM-MDM)-based FSO transceiver was described in cite 10. Signal to-noise-ratio (SNR) and total power are used as the main measuring variables to quantify the dust effect. For FSO linkages, the effect of sandstorm conditions was examined in [16]. The performance of the backhaul network, which was introduced in [17] for a 5G-based FSO system is assessed and contrasted with that of a traditional FSO link. Reference [18] looked into the function of the FSO framework in the next-generation satellite communication system. The COVID-19 epidemic, on the other hand, has offered an increase to online application and marketing services, overtaxing the already deployed FSO setups. To increase capacity and transmission accuracy, the combined optical network and FSO structure are presented in this study utilizing 5G NR and sub-THz based 64QAM-OFDM signals.

The structure of this manuscript is as follows. The analytical inquiry is presented in Section 2, the proposed experimental setup is described in Section 3, the experimental measurements and analysis are covered in Section 4, and the combined fiber-FSO model is summarised in Section 5.

2. Theoretical Investigations of Proposed Fiber-FSO System

The mixed FSO and fiber link system is introduced in this paper, purposing to minimize the nonlinear issues and FSO related impairments like RF alignment issues, FSO pointing errors, and cochannel interference. This section includes the analytical calculations for the proposed FSO and optical systems. The channel model of FSO is defined [14, 15] as follows:

$$F_{ch} = \psi_a \psi_p \psi_l, \tag{1}$$

where the F_{ch} presents the FSO channel, ψ_a, is the atmospheric turbulence loss, ψ_l is the geometric loss, and the ψ_p is the FSO pointing issues. Three components are considered for optical signal transmission [16]. (1) Line of sight component. (2) Line of sight coupled with the scattered component. (3) Independent scattered component. The power distribution function (pdf) for free space is expressed [17–20] as follows:

$$f_{F_{ch}}(F_{ch}) = B\sum_{n=1}^{\beta_m} a_n F_{ch}^{\alpha_m+n/2-1} N_{\alpha-n}\left(2\sqrt{\frac{\alpha_m\beta_m F_{ch}}{\gamma\beta_m + P'}}\right), \quad (2)$$

and B means

$$B = \frac{2\alpha_m^{\alpha_m/2}}{\gamma^{1+\alpha_m/2}\varphi(\alpha_m)}\left(\frac{\gamma\beta_m}{\beta_m + P'}\right)^{\beta_m+\alpha_m/2}, \quad (3)$$

where α_m is the large scale scattering process, β_m is the fading parameter, γ is the independent scattering component, and $\varphi(.)$ represents gamma function. The p' is defined as follows:

$$p' = p + 2\tau b_0, \quad (4)$$

where the p is the power for the first line of sight component and $2\tau b_0$ is the coupled line of sight and scattered component. The parameter a_n is further explain [21] as follows:

$$a_n = \begin{bmatrix}\beta_m - 1\\ n-1\end{bmatrix}\frac{(\gamma\beta_m + p')^{1-n/2}}{(n-1)!}\left(\frac{p'}{U}\right)^{n-1}\left(\frac{\alpha_m}{\beta_m}\right)^{n/2}, \quad (5)$$

where β_m is the fading element, α_m is the effective number of large scale scattering process. The FSO system performance is conditioned by the transceiver and structural ways; this leads to FSO pointing impairments, and it is calculated in terms of PFD [22, 23] as follows:

$$f_{\psi_p} = \frac{u^2}{A_0^{u^2}}(\psi_p)^{u^2-1}, \quad 0 \le \psi_p \le A_0, \quad (6)$$

where A_0 is integrated optical power function, u is related to jitter deviation and equal to $\omega_z/2\sigma^2$. The width of the data carrying laser beam is denoted by ω_z. The statistical analysis of FSO pointing errors, turbulence fading, and cochannel interference is expressed [24, 25] as follows:

$$f_{F_{ch}}(F_{ch}) = \int f_{F_{ch}/\psi_a}\left(\frac{F_{ch}}{\psi_a}\right).f_{\psi a}(\psi_a)d\psi_a. \quad (7)$$

In equation (6) the $f_{F_{ch}/\psi_a}(F_{ch}/\psi_a)$ declares the conditional probability. By substituting equation (1) to equation (5) in equation (6), the CDF of the N channel is defined as follows:

$$f_{F_{ch}}(F_{ch}) = \frac{u^2 B}{2}\sum_{n=1}^{\beta_m}\left(a_n\left[\frac{1}{A_m}\right]^{\alpha+n/2}\right)G_{2,4}^{3,1}\left(\frac{F_{ch}}{AB_0 I_l}\right), \quad (8)$$

where $G_{2,4}^{3,1}$ is the Meijer's G function. On the transmitter side, multipulse position modulation (MPPM)-based intensity modulation direct detection system is used for the FSO system. The electrical filter is installed on the receiver side to remove unwanted signals from the original signals. The output of the filtered signal is calculated as follows:

$$y(t) = R\frac{N}{n}P_R\sum_{n=0}^{N-1} C_n + k(t). \quad (9)$$

The average received optical power, R is the photodetector responsivity, $k(t)$ is the additive white Gaussian (AWG), and C_n is the signal time slot. The transmitter and receiver telescope gains are expressed [18, 26, 27] as follows:

$$G_t = G_r = \left(\frac{\pi d}{\lambda_k}\right)^2. \quad (10)$$

G_t is the transmitter gain, G_r is the receiver gain, and d is the diameter. The receiver signal to noise ratio (SNR) of the FSO system is estimated as follows:

$$\mathrm{SNR}(F_{ch}) = R^2 P_t^2\left(\frac{\eta B_r}{\lambda_k L}\right)^4\frac{\mathrm{Modlog_2\,Mod}}{2M\sigma_n^2}F_{ch}. \quad (11)$$

σ is the variance of channel noise, η is the efficiency, Mod is the modulation order, and M is the number of transceivers. The conditional probability error of the presented integrated optical network and FSO system is calculated as follows:

$$\mathrm{BER}(F_{ch}) = \frac{\mathrm{Mod}}{4}erfc\left[Rp_R(F_{ch})\frac{\sqrt{\mathrm{Modlog_2Mod}}}{2\sigma_k}\right], \quad (12)$$

where $erfc$ is the error function. The outage probability of the fading channel is calculated as

$$p_{\mathrm{out}} = p(\mathrm{SNR}) \le \mathrm{SNR}. \quad (13)$$

3. Experimental Setup

This section discusses the experimental background of the presented model, which is depicted in Figure 2. The sub-THz based 5G NR signals are linked with a 25 km single-mode fiber (SMF) and a 500 m FSO link. The principle operation of fiber-FSO is like this: an optical comb of coherent carriers is induced with 25 and 50 GHz spacing and passed over the erbium-doped fiber amplifier (EDFA), fulfilling the amplification need. Then the signals are divided through an optical divider and injected into an optical bass pass filter (OBPF) which has a 0.7 nm bandwidth and an 800 dB/nm filter slope. These filtered optical signals are credited to the mach Zender modulator (MZM) (40 GHz capacity), and in parallel, the 64 QAM-OFDM waves are produced at 22 Gbps bit speed and transformed by the same MZM. The process of generating 64QAM-OFDM signals includes a serial to parallel (S/P) converter, a cyclic prefix (CP), symbol mapping, a parallel to serial converter (P/S), digital to analogue conversion (DAC), and the inverse fast Fourier transform (IFFT). Adding to the 64 OFDM process, the conjugate symmetric data are added prior to the IFFT function. The modulated data are propagated over SMF after amplification and passed through an attenuator. The split signals are then

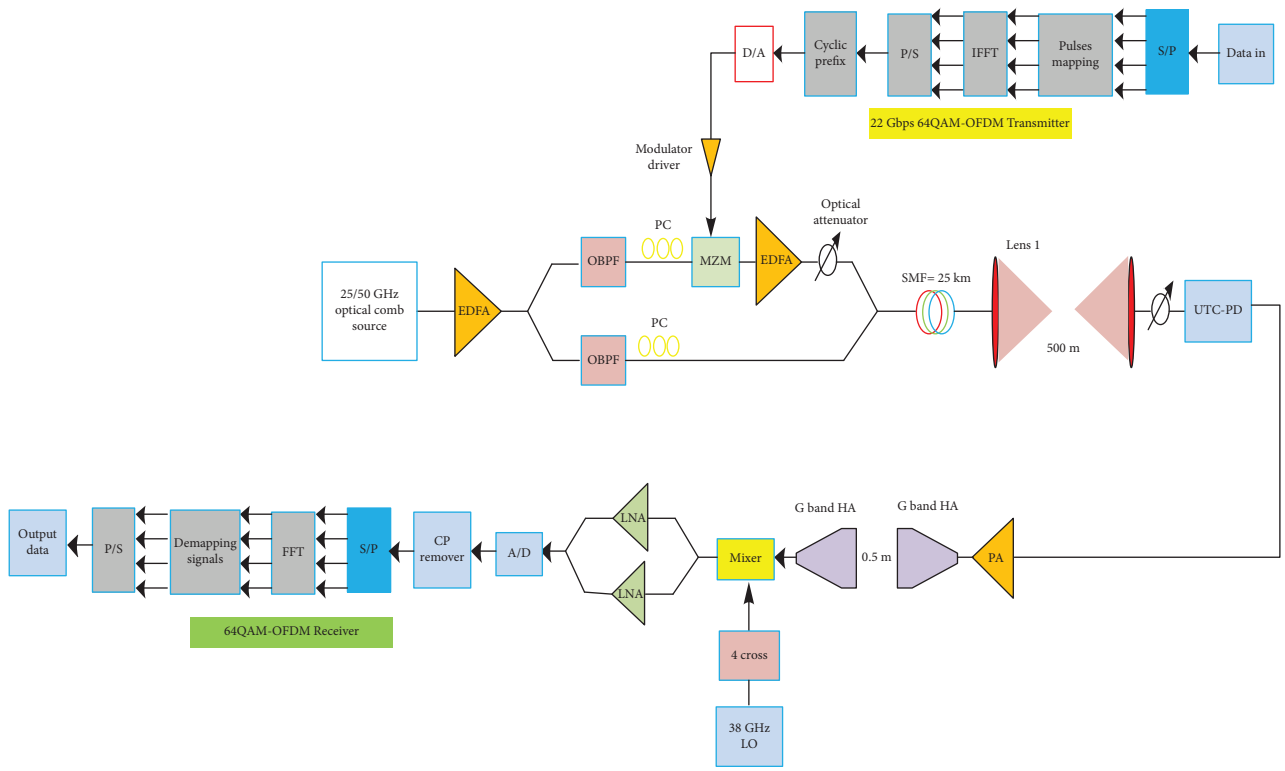

Figure 2: 5G NR based united fiber and FSO framework.

combined by using an optical coupler (2×1) and outputs are loaded into the double lens-based FSO system (500 m, AC508), including convex and concave lenses. After covering the 500 m area of the FSO system, the signals are detected by a uni travel photodiode (UTC-PD) consisting of optical carriers and local oscillator waves. The received electrical signals are then amplified using a power amplifier (PA), and the G-band horn antenna (HA) is installed after the PA, aiming to remove unwanted beat frequencies. On the output side of the 5 m RF system, a mixer is connected to downconvert the sub-THz signals into a lower frequency range. In the next process, the downconverted signals are further purified through low-noise amplification (LNA), which consists of a 3.8 dB noise figure and an 18–40 GHz frequency range. In the final step, the 64QAM-OFDM demodulation is linked to the end side of the presented fiber FSO system. This block contains all the key parameters, such as P/S and S/P converters, QAM demapper, CP removal, FFT, and ADC. Table 1 includes the list of elements applied for analyzing the performance the proposed fiber-FSO system.

4. Experimental Measurements and Analysis

The presented joint model of giber and FSO is evaluated experimentally in this section. The features of the suggested model are extracted in graphical presentation and described, along with the performance of the 5G NR sub-THz-based fiber-FSO system as compared to current approaches. Figure 3 introduces the results estimation regarding received optical power and BER, which compares the outlets among

Table 1: Parameters range with units applied for analyzing 5G NR based fiber-FSO system performance.

Name of the element	Description of the element
Transmitted	64QAM-OFDM
SMF length	25 km
FSO space	500 m
RF range	0.5 m cascaded media
UTC-PD size	250 GHz
Data rate	22 Gbps
5G NR sub-THz signal format	125–200 GHz/22 Gbps
Noise figure	3 dB

5G NR sub-THz fiber-FSO system and conventional fiber-FSO system using clear and poor weathers conditions. It is clarified that the efficacy of the presented 5G NR-based fiber FSO framework is far better than the conventional model, even in poor weather conditions. If we investigate the difference among proposed model and traditional fiber-FSO model in terms of BER points, the achievements of 5G NR based fiber-FSO system in poor weather are 5 points reliable than the achievements of standard fiber-FSO system even in clear weather situations.

The results of the performance of UTC-PD in terms of relative response (dB) and frequency (GHz) are discussed in Figure 4, showing that the relative response of the presented model decreases with increasing the frequency range. The high-bandwidth UTC-PD has attractive performance at high-frequency response for a combined fiber-FSO system. The bandwidth above 250 GHz is considered suitable for

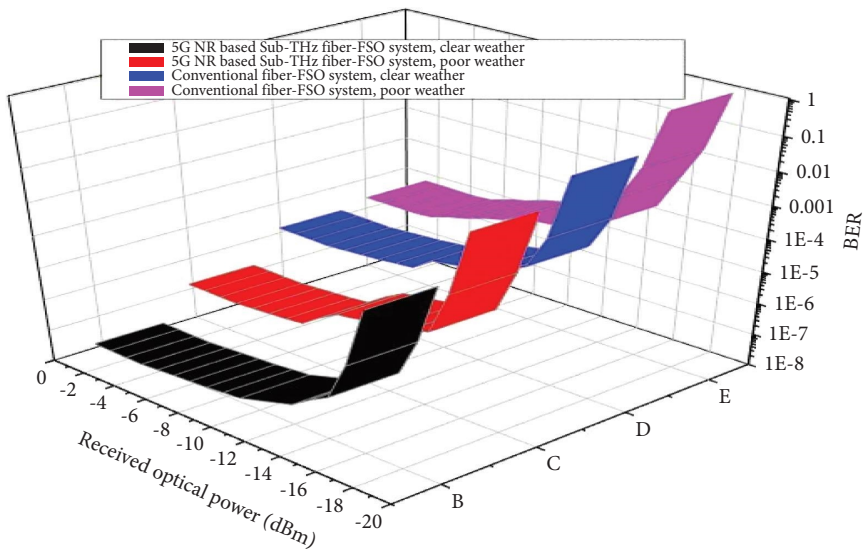

Figure 3: Comparison investigation of presented fiber-FSO setup and conventional fiber-FSO system using BER and received optical power in dBm.

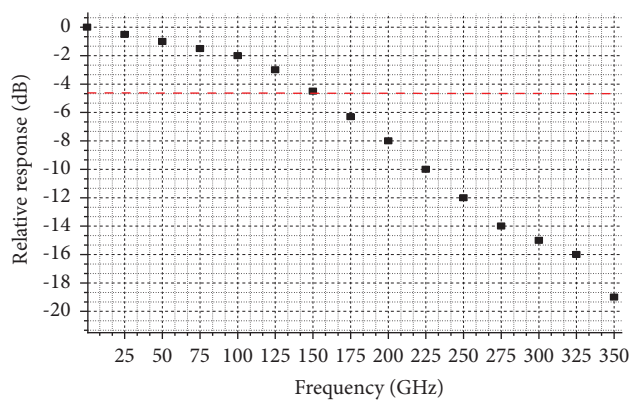

Figure 4: Frequency measurements as a function of relative response.

UTC-PD to act as an optical detector and convert the optical signal into electrical form at the receiver side. Furthermore, the proposed 5G NR based fiber-FSO system calculations are investigated for different frequency ranges of sub-THz (125, 150, 175, and 200 GHz), as highlighted in Figure 5, applying 22 Gbps data rate speed with EVM and SNR measuring parameters. It is shown that by enhancing the range of 64QAM-OFDM signal frequency, the performance of the system is disturbed as compared to 125 and 150 GHz signal frequencies. The EVM 14% range is observed by 125 GHz-based 64QAM-OFDM signal earlier (19 dB) than 150, 175, and 200 GHz signal frequency (21.2, 21.8, and 24 dB, respectively). This performance of the presented fiber-FSO system was studied at 25 km SMF length, 500 m FSO volume, and 0.5 m RF cross-media range.

In Figure 5, the experimental investigations are done for 20 and 25 GHz bandwidth and 100, 150, and 200 GHz 64QAM-OFDM signal frequencies at a 22 Gbps data rate. The results show fruitful achievements at 25 GHz bandwidth; the EVM threshold line is touched at −30 dBm. On the other side, it is evaluated that with increasing the signal frequency range, the performance of fiber-FSO is degraded because of high-capacity signals; however, at maximum output power, the position of fiber-FSO can be balanced against high-data rate transmission, as shown in Figure 6. In addition, three types of 64QAM-OFDM signal frequencies (100, 150, and 200 GHz) are tested in Figure 6 at 22 Gbps, and 25 km SMF length, which describes the efficient outlets for all frequency ranges and bandwidths. Similarly, in Figures 7 and 8 the exhibitions of the 100 GHz signal-based channel of the fiber-FSO system and the actions of the generated 64QAM-OFDM signals, respectively.

In final discussion of the experimental analysis, Figure 9 presents the constellation diagram measurements of the proposed 5G NR based fiber-FSO system and conventional fiber-FSO system, where Figure 9(a) declares the constellation analyzer of the input 64QAM-OFDM signals, Figure 9(b) demonstrates the constellation conductions of 5G NR-based proposed fiber-FSO system at 25 km SMF, 150 GHz/22 Gbps capacity with 500 m FSO and 0.5 m RF

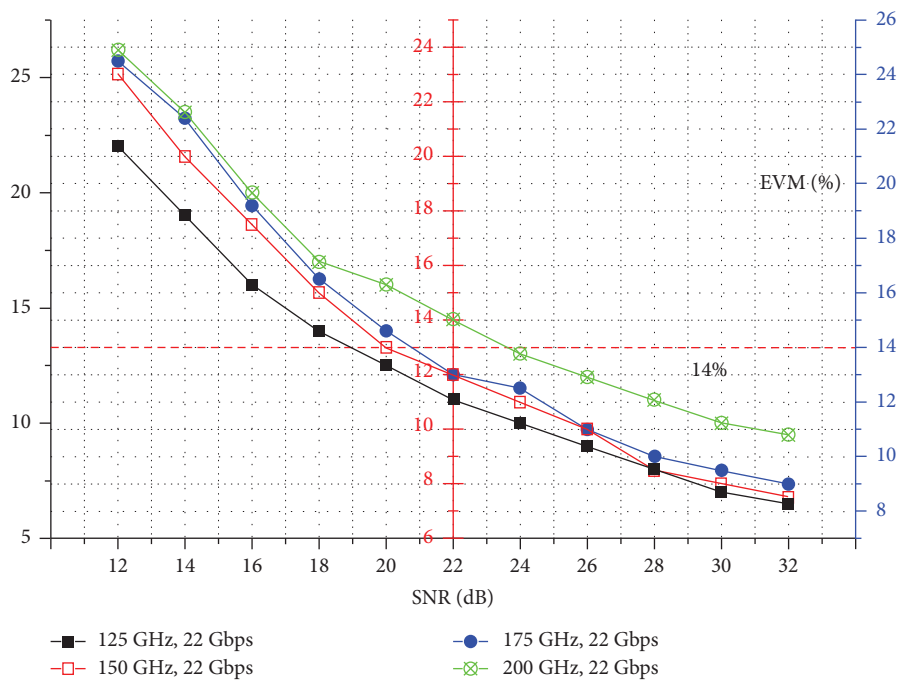

Figure 5: Various sub-THz signals measurements for evaluating integrated fiber-FSO efficiency.

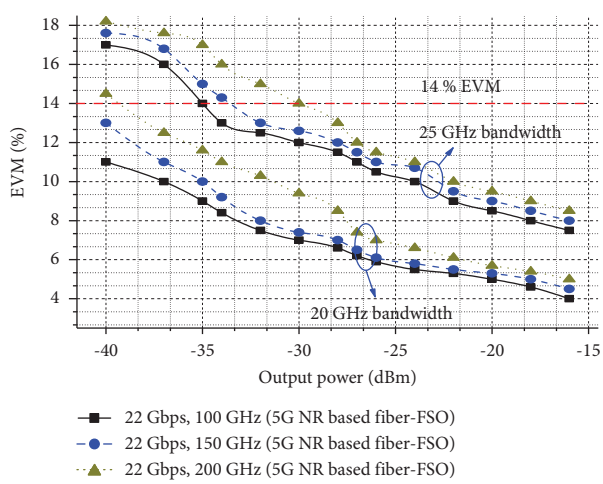

Figure 6: Received power against EVM analysis for different bandwidths and 64QAM-OFDM signal frequencies.

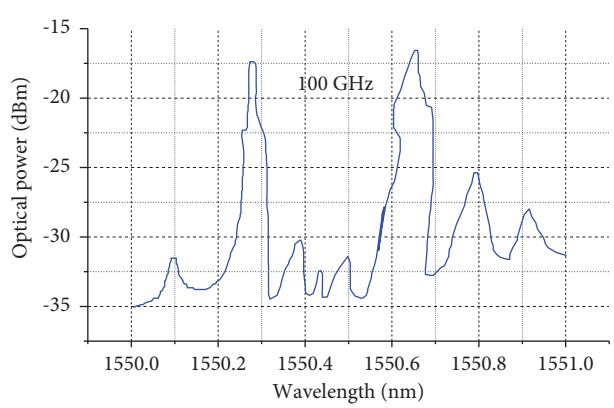

Figure 7: Optical power estimations at different wavelengths.

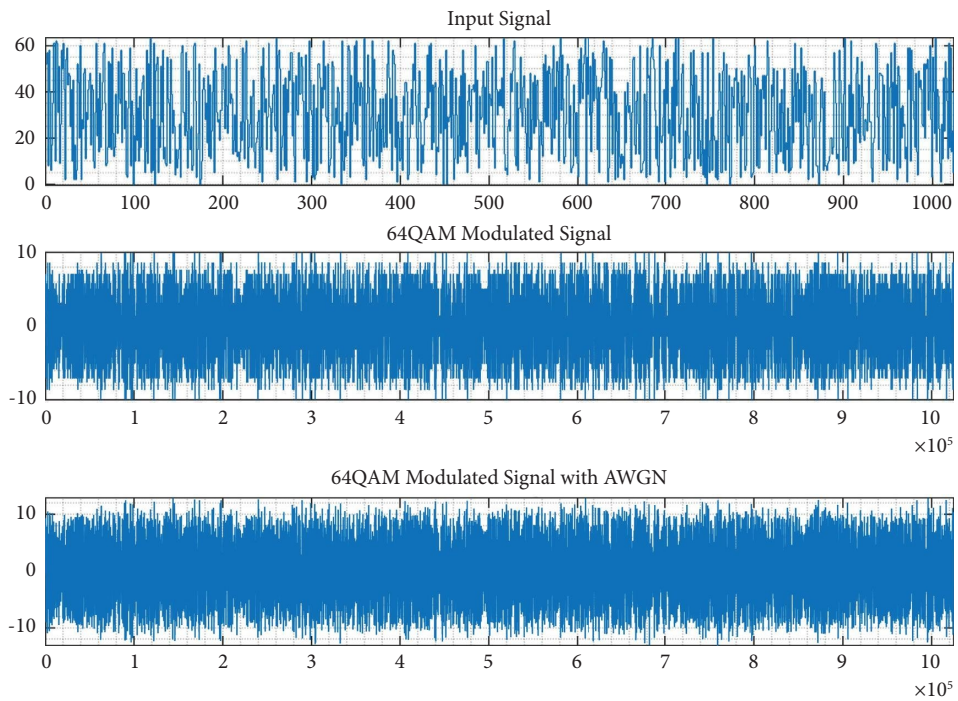

Figure 8: Status of generated 64QAM-OFDM signals and input signals.

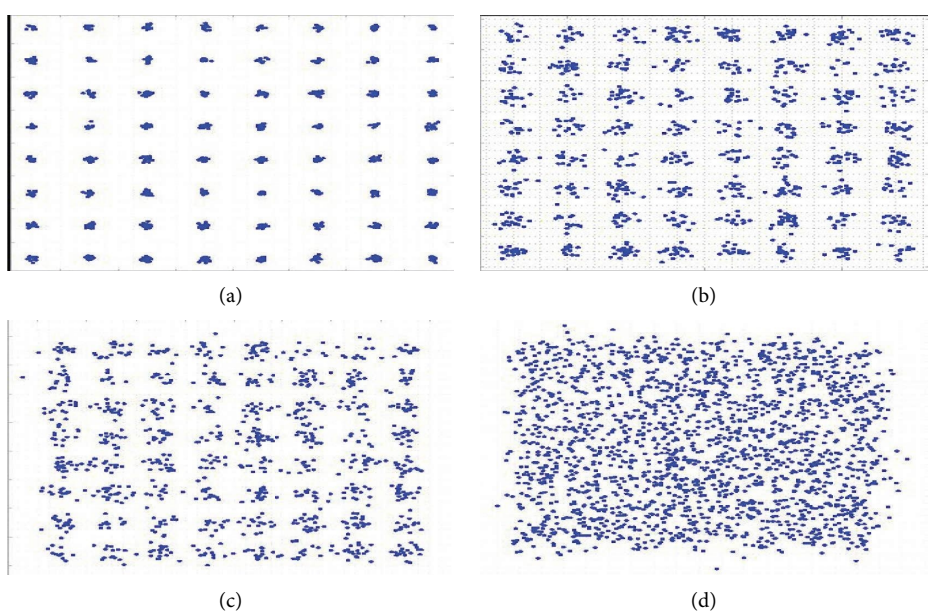

Figure 9: Constellation diagram estimations. (a) The position of the 64QAM-OFDM signals at input side. (b) The performance of the 5G NR-basedfiber-FSO system at 150 GHz/22 Gbps at 25 km SMF. (c) The outcomes achievements of the 5G NR-basedfiber-FSO system at 200 GHz/22 Gbps and 25 km SMF. (d) The performance of the convectional fiber-FSO system at 25 km SMF and 150 GHz/22 Gbps.

wireless range, Figure 9(c) discusses the constellation outputs of the proposed 5G NR-basedfiber-FSO system at 25 km SMF, 200 GHz/22 Gbps capacity with 500 m FSO and 0.5 m RF media, and last Figure 9(d) shows the outcomes of the conventional fiber-FSO model at 150 GHz/22 Gbps and 25 km SMF.

5. Conclusion

The 5G NR sub-THz-based integrated fiber and FSO system is designed and evaluated for high capacity range transmission, including 500 m FSO and 0.5 RF mediums. The presented model is carried out using mathematical structure

using the valid and real-based parameters like input power range, signal frequency of 64QAM-OFDM, and received power and length of SMF. After the detailed discussion on the mathematical framework, the experimental analysis are then measured and compared with the conventional fiber-FSO system. The experimental results are studied using various signal frequency ranges like 125,150, 175, and 200 GHz, received power, relative response of UTC-PD, 500 FSO medium, and 0.5 m RF wireless medium. In correlation with the conventional fiber-FSO system it is concluded that the results investigations that the presented model has efficient and reliable outlets even at high capacity channel transmissions. In future studies, we can add the updated machine learning model to further smooth the flow of signals and minimize high-order noises including phase and nonlinear impairments.

Data Availability

The data are available in this paper.

Conflicts of Interest

The authors declare that they have no conflicts of interest.

References

[1] X. Zhao, L. Zhu, S. Fu, C. Liu, M. Tang, and D. Liu, "Dual-band accelerating beams enabled full duplex free-space optical interconnection," *IEEE Journal of Selected Topics in Quantum Electronics*, vol. 27, no. 1, 2021.

[2] H. Yu, F. Ali, S. Tu et al., "Deducing of optical and electronic domains based distortions in radio over fiber network," *Applied Sciences*, vol. 12, no. 2, p. 753, 2022.

[3] S. Rahman, F. Ali, A. Smagor et al., "Mitigation of nonlinear distortions for a 100 Gb/s radio-over-fiber-based WDM network," *Electronics*, vol. 9, no. 11, p. 1796, 2020.

[4] T. J. Jabeena and R. Aggarwal, "Review on optimization of wireless optical communication system," *Trends in Opto-Electro & Optical Communications*, vol. 4, pp. 9–19, Apr. 2019.

[5] H. Singh, N. Mittal, R. Miglani, H. Singh, G. S. Gaba, and M. Hedabou, "Design and analysis of high-speed free space optical (FSO) communication system for supporting fifth generation (5G) data services in diverse geographical locations of India," *IEEE Photonics Journal*, vol. 13, no. 5, pp. 1–12, Oct. 2021.

[6] J. M. C. Brito, L. L. Mendes, and J. G. S. Gontijo, "Brazil 6G project-an approach to build a national-wise framework for 6G networks," in *Proceedings of the 2nd 6G Wireless Summit (6G SUMMIT)*, pp. 1–5, Levi, Finland, March 2020.

[7] M. Kamal, J. Khan, Y. Khan et al., "Free space optics transmission performance enhancement for sustaining 5G high capacity data services," *Micromachines*, vol. 13, no. 8, p. 1248, 2022.

[8] F. Muhammad, F. Ali, U. Habib, M. Usman, I. Khan, and S. Kim, "Time domain equalization and digital back-propagationmethod-based receiver for fiber optic communication systems," *International Journal of Optics*, vol. 2020, pp. 1–13, Article ID 3146374, 2020.

[9] F. Ali, F. Muhammad, U. Habib, Y. Khan, and M. Usman, "Modeling and minimization of FWM effects in DWDM-basedlong-haul optical communication systems," *Photonic Network Communications*, vol. 41, no. 1, pp. 36–46, 2020.

[10] A. S. Hamza, J. S. Deogun, and D. R. Alexander, "Classification framework for free space optical communication links and systems," *IEEE Commun. Surveys Tuts.*vol. 21, no. 2, pp. 1346–1382, 2019.

[11] M. A. Esmail, A. M. Ragheb, H. A. Fathallah, M. Altamimi, and S. A. Alshebeili, "5G-28 GHz signal transmission over hybrid all-optical FSO/RF link in dusty weather conditions," *IEEE Access*, vol. 7, pp. 24 404–424 410, 2019.

[12] A. O. Mufutau, F. P. Guiomar, M. A. Fernandes, A. Lorences-Riesgo, A. Oliveira, and P. P. Monteiro, "Demonstration of a hybrid optical fiber–wireless 5G fronthaul coexisting with end-to-end 4G networks," *Journal of Optical Communications and Networking*, vol. 12, no. 3, pp. 72–78, Mar. 2020.

[13] C.-Y. Li, X.-H. Huang, H.-H. Lu, Y.-C. Huang, Q.-P. Huang, and S.-C. Tu, "A WDM PAM4 FSO-UWOC integrated system with a channel capacity of 100 gb/s," *Journal of Lightwave Technology*, vol. 38, no. 7, pp. 1766–1776, 2020.

[14] E. S. Lima, R. M. Borges, L. A. Melo Pereira, H. R. Dias Filgueiras, A. M. Alberti, and A. Cerqueira Sodre, "Multiband and photonically amplified fiber-wireless xhaul," *IEEE Access*, vol. 8, pp. 44381–44390, 2020.

[15] J. Zhao, Y. Liu, and T. Xu, "Real-time phase delay compensation of PGC demodulation in sinusoidal phase-modulation interferometer for nanometer displacement measurement," *Journal of Applied Sciences*, vol. 9, no. 19, p. 4192, 2019.

[16] A. Jahid, M. H. Alsharif, and T. J. Hall, "A contemporary survey on free space optical communication: potentials, technical challenges, recent advances and research direction," *Journal of Network and Computer Applications*, vol. 200, Article ID 103311, 2022.

[17] R. Li, B. Lin, Y. Liu, M. Dong, and S. Zhao, "A survey on laser space network: terminals, links, and architectures," *IEEE Access*, vol. 10, pp. 34815–34834, 2022.

[18] X. Liu, J. Fang, S. Xiao, L. Zheng, and W. Hu, "Adaptive probabilistic shaping using polar codes for FSO communication," *IEEE Photonics Journal*, vol. 14, no. 1, pp. 1–6, 2022.

[19] M. Z. Chowdhury, M. Shahjalal, S. Ahmed, and Y. M. Jang, "6G wireless communication systems: applications requirements technologies challenges and research directions," *IEEE Open J. Commun. Soc.,*vol. 1, pp. 957–975, 2020.

[20] Payal and S. Kumar, "Free Space Optics: a shifting paradigm in optical communication systems in difficult terrains," in *Proceedings of the Ist Int. Conf. on Sustainable Technologies for Computational Intelligence*, pp. 537–550, Berlin, Germany, 2020.

[21] M. K. Arti and A. Jain, "A simple approximation of FSO link distribution and its applications," in *Proceedings of the 2020 IEEE International Conference on Advanced Networks and Telecommunications Systems*, pp. 1–3, ANTS, New Delhi, India, December 2020.

[22] F. V. Corral, C. Cuenca, and I. Soto, "Design of an optical wireless network using free space optics technology (FSO), in 5G/6G networks environment," in *Proceedings of the Proc. IEEE Intl Conf. Autom./XXIV Congr. Chil. Assoc. Automat. Contr*, pp. 1–5, Valparaíso, Chile, March 2021.

[23] M. N. Thi, V. Mai, and H. Kim, "Seven-aperturedirect-detection receiver for free-space optical communication systems," in *Proceedings of the 2022 Optical Fiber Communications Conference and Exhibition (OFC)*, pp. 1–3, San Diego, CA, USA, March 2022, https://ieeexplore.ieee.org/document/9748748.

[24] H. H. Lu, X. H. Huang, W. S. Tsai et al., "800 Gb/s/200 m FSO link with a WDM-PAM4 scheme and SLM-based beam tracking technology," *Optics Letters*, vol. 46, no. 6, pp. 1269–1272, 2021.

[25] V. Akbucak, G. Aymelek, B. Yolcu et al., "Effect of partial coherence on signal-to-noise ratio performance of free space optical communication system in weak turbulence," *Optics Communications*, vol. 518, Article ID 128395, 2022.

[26] G. Wang, L. Y. Shao, D. Xiao et al., "Stable and highly efficient free-space optical wireless communication system based on polarization modulation and in-fiber diffraction," *Journal of Lightwave Technology*, vol. 39, no. 1, pp. 83–90, Jan. 2021.

[27] Y. Wu, *6G Mobile Wireless Networks*, Springer Nature Switzerland AG, Berlin, Germany, 2021.